



HAL
open science

Rotational/compressional nature of the magnetopause: Application of the BV technique on a magnetopause case study

Nicolas Dorville, Gérard Belmont, Laurence Rezeau, Roland Grappin,
Alessandro Retinò

► To cite this version:

Nicolas Dorville, Gérard Belmont, Laurence Rezeau, Roland Grappin, Alessandro Retinò. Rotational/compressional nature of the magnetopause: Application of the BV technique on a magnetopause case study. *Journal of Geophysical Research Space Physics*, 2014, 119, pp.1898-1908. 10.1002/2013JA018927 . hal-01552017

HAL Id: hal-01552017

<https://hal.science/hal-01552017>

Submitted on 5 Mar 2024

HAL is a multi-disciplinary open access archive for the deposit and dissemination of scientific research documents, whether they are published or not. The documents may come from teaching and research institutions in France or abroad, or from public or private research centers.

L'archive ouverte pluridisciplinaire **HAL**, est destinée au dépôt et à la diffusion de documents scientifiques de niveau recherche, publiés ou non, émanant des établissements d'enseignement et de recherche français ou étrangers, des laboratoires publics ou privés.

1 Rotational/ Compressional nature of the
2 Magnetopause: application of the BV technique on a
3 magnetopause case study

Nicolas Dorville,¹ Gérard Belmont,¹ Laurence Rezeau,¹ Roland Grappin,¹

Alessandro Retinò,¹

arXiv:1304.1412v1 [astro-ph.EP] 4 Apr 2013

Corresponding author: N. Dorville, LPP, Ecole Polytechnique, CNRS, UPMC, Université Paris Sud, Palaiseau, France.(nicolas.dorville@lpp.polytechnique.fr)

¹LPP, Ecole Polytechnique, CNRS,
UPMC, Université Paris Sud, Palaiseau,
France

4 Abstract.

5 The magnetopause boundary implies two kinds of variations: a density/
6 temperature gradient and a magnetic field rotation. These two kinds are al-
7 ways observed in a close vicinity of each other, if not inseparably mixed. We
8 present a case study from the Cluster data where the two are clearly sep-
9 arated and investigate the natures of both layers. We evidence that the first
10 one is a slow shock while the second is a rotational discontinuity. The inter-
11 action between these two kinds of discontinuities is then studied with the help
12 of 1,5-D magnetohydrodynamics simulations. The comparison with the data
13 is quite positive and leads to think that most of the generic properties of the
14 magnetopause may be interpreted in this sense.

1. Introduction

15 The Earth magnetopause is the outer boundary of the terrestrial magnetosphere. Out-
16 side of this boundary, the magnetosheath plasma is the shocked solar wind plasma, *i.e.*
17 cold and dense, with a magnetic field direction essentially determined by the solar wind
18 one. Inside of it, the magnetospheric plasma is hot and tenuous, with a magnetic field
19 direction essentially determined by the planetary one. For this reason, two kinds of strong
20 gradients are observed in the same close vicinity: a compressional one (density, temper-
21 ature and possibly magnetic and kinetic pressures) and a rotational one (magnetic field
22 direction). Understanding how these two kinds of variations can co-exist is a pivotal issue
23 for understanding the nature of the boundary. Whenever this boundary can be locally con-
24 sidered as stationary and one-dimensional, the Rankine-Hugoniot jump equations allow
25 only one type of discontinuity able to ensure simultaneously the two kinds of variations:
26 the tangential discontinuity. It implies that the normal magnetic field and flow are equal
27 to zero in the frame of the discontinuity.

28 There is now observational evidence (*Chou et al*, 2012) that the magnetopause is not al-
29 ways a tangential discontinuity, *i.e.* that the normal flow and magnetic field are not always
30 null. There are in particular numerous observations where the magnetic field rotation cor-
31 responds to a rotational discontinuity (*Sonnerup et al*, 1974). In this paper, we use the
32 word "discontinuity" in its usual sense in this context: a 1-D stationary layer, whatever its
33 thickness. It seems that, at least when dynamical processes takes place (due for instance
34 to reconnection near the studied site), the compressional boundary and the rotational one
35 can be distinguished, both propagating with different velocities with respect to the flow.

36 Our goal is to present evidence of such a case with a detailed experimental analysis and
37 suggest an interpretation of the observations. In sections 2 to 4, the experimental Clus-
38 ter case is presented and the two crossings are analyzed with the help of a new method
39 presented in [Dorville *et al*, submitted to JGR 2013]. In section 5, the interaction of a
40 compressional jump and a rotational one is investigated by solving numerically the MHD
41 equations, in order to understand to what extent the properties of both are modified by
42 the interaction, in particular their propagation speeds. The comparison with the data
43 and the conclusions are drawn in section 6.

2. Study of a magnetopause crossing by Cluster

44 Using the single-spacecraft method of analysis described in (Dorville *et al*, submitted
45 to JGR, 2013) we are able to build a one-dimensional spatial transition parameter at the
46 magnetopause and to analyze the small scales inside the boundary during a magnetopause
47 crossing. This new transition parameter is expectingly close to a normal linear coordi-
48 nate. The assumptions of the method is that the boundary is one-dimensional, sufficiently
49 stationary during the crossing, and that the speed of the flow in its frame is negligible
50 with respect to the speed of the boundary. A fit of the two temporal tangential field
51 components with a spatial elliptic form is done, in the frame where the normal magnetic
52 field is constant and where the normal speed of the flow is consistent with an angle on
53 the ellipse linear with spatial position.

54

55 In this part we focus on a magnetopause crossing by Cluster C1 on April 15th 2008,
56 between 15:19:05 and 15:25:05. Fig. 1 shows the variation of ion density obtained by the
57 Hot Ion Analyzer (HIA), the energy spectrum, and the variation of the Fluxgate Magne-

58 tometer (FGM) magnetic field (*Balogh et al, 1997*) associated with this crossing.

59 For this magnetopause crossing, we are able to fit the magnetic field and find a transition
60 parameter consistent with CIS (*Rème et al, 1997*) ion velocity. The observed angle on the
61 ellipse as a function of time (in black) and the angle derived by the fit with CIS velocity
62 (in red) are plotted on Fig. 2. The fit is good on this case. The method also provides
63 an accurate determination of the normal direction, which is here slightly different from
64 the MVABC [Minimum and Maximum Variance Analysis] one: ([0.98,-0.18,-0.10] against
65 [0.96, -0.10, 0.25] in GSE coordinates). The result of the fit on magnetic field is presented
66 on Fig. 3, where time zero is the center of the large data interval and the fit is done on the
67 time period of the magnetic field rotation. It is worth noticing that the variance on B_m
68 is not much larger than the variance on B_n , which makes the MVAB method inefficient.
69 On the other hand, MVABC assumes that $B_n = 0$, which does not allow determining it
70 either. Our method provides a value $B_n = 14nT$, corresponding to a propagation angle
71 $\theta_{Bn} = 75$ degrees .

72

73 Looking inside the boundary, Fig. 4 presents the time evolution of density, total magnetic
74 field and B_z . It seems clear that there are two phases in the evolution of these quantities:
75 first, the density is rapidly increasing and the magnetic field amplitude B is decreasing.
76 Then, these quantities remains constant and the magnetic field slowly rotates on an el-
77 lipse. We will now study these two phases separately, assuming they are oriented along
78 the same normal direction.

3. Compressional variations

79 Let us first focus on the first, compressional, phase, between $t=-9$ and $t=2$, when the
 80 density is growing and the total field decreasing. The first step to study this discontinu-
 81 ity is to find its normal velocity, in order to work in its proper frame. We cannot here
 82 make the simple assumption that the observed velocity is the boundary velocity because
 83 this layer is compressional and there is certainly, according with the conservation of the
 84 flux, a consistent velocity gradient inside the boundary. To determine the velocity of the
 85 boundary using the mass conservation, we plot the measured ion flux ρu_n relatively to
 86 the measured density ρ Fig. 5, for the three CIS measurement points available inside the
 87 shock, altogether with the nearest points around the shock. This flux has to be constant
 88 in the frame on the boundary, and its variation must be proportional to the velocity of
 89 the boundary in another frame. We find that the points are aligned with a constant
 90 flux of $1.07 \pm 0.11 \cdot 10^{11}$ (SI) and a velocity of the boundary of 55.1 ± 1 Km/s, the given
 91 uncertainties being the 1-sigma uncertainties estimated from the fits. If we restrict to the
 92 only three points in the gradient, we find that the points are perfectly aligned with a flux
 93 of $1.09 \pm 0.01 \cdot 10^{11}$ (SI) and a velocity of the boundary of 54.7 ± 0.1 km/s.

94

95 Here we have to notice that if we look at the same points on MVABC frame or MVAB
 96 frame, the flux is not proportional to the density. So the precision of the frame found with
 97 our method seems to be better, that is very important for such a precise treatment. Even
 98 with the small numbers of CIS points, we can be confident on this value and work on the
 99 discontinuity frame. Fig. 6 represents the variation of density, pressure, field modulus
 100 and normal velocity. We see that the last two quantities decrease as the others increase,

101 that is possible only for a slow shock with respect to the Rankine-Hugoniot equations.
102 Indeed, we find that the flow is super-slow on magnetospheric side and sub-slow on the
103 other side, as the Cs on the curve refers to the slow mode velocity. So this discontinuity
104 can be identified with confidence as a slow shock.

4. Rotational variations

105 Fig. 7 shows the second part of this magnetopause crossing. The plotted quantities are
106 the density, temperature, pressure and magnetic field. All seem to be constant in this
107 part of the boundary, with only a slow rotation of the direction of magnetic field. It is
108 also the case for the velocity modulus. These evolutions are characteristic of a rotational
109 discontinuity.

110 To test this discontinuity, we used a variant of the Walen test (*Paschmann et al*, 2008)
111 on Fig. 8. We plot the variations δB_t as a function of $\sqrt{(\mu_0\rho)} \delta u_t$ for the two tangential
112 components. The result appears consistent with a rotational discontinuity, but with a
113 little difference: the slope is not equal to one as it should, but to about 0.72, 0.74 with
114 the correction coming from the temperature anisotropy at this place. To explain it from
115 the composition of the plasma, we would need a mean mass of 1.8 protons. Unfortunately
116 there is no CODIF data for C1 on April 15th, and no good resolution electron density
117 measurement.

118

119

5. Direct numerical simulations of a slow-shock/rotational discontinuity interaction

Let us now consider the hypothesis that this magnetopause crossing is the observation of a non stationary interaction between an Alfvén wave and a slow shock. This model should enable to describe many observations of the magnetopause, since both a compression and a rotation of \mathbf{B} have to be present. In order to investigate this possibility, we use a one-dimensional MHD simulation code.

5.1. Initialisation of the shock

We use a 1.5 D compressible MHD simulation code with periodic boundary conditions. The code uses a classical Fourier pseudo-spectral method to compute spatial derivatives, with an adaptive second order Adams-Bashforth time stepping for time integration. We integrate the equations for the density ρ , the gas pressure P , the velocity u , and the magnetic field B . The temperature is defined by an ideal gas law. These equations read, appropriately normalized:

$$\partial_t \rho + \nabla \cdot (\rho u) = 0 \quad (1)$$

$$\partial_t P + (u \cdot \nabla) P + \gamma P \nabla \cdot u = D_1 \quad (2)$$

$$\partial_t u + (u \cdot \nabla) u + \nabla(P + B^2/2)/\rho - (B \cdot \nabla) B/\rho = D_2 \quad (3)$$

$$\partial_t B + (u \cdot \nabla) B - (B \cdot \nabla) u + B \nabla \cdot u = D_3 \quad (4)$$

$$P = \rho T \quad (5)$$

D_2 and D_3 denote respectively the viscous and resistive dissipative terms, and D_1 the corresponding heating terms, together with conduction. Only plane waves are considered, *i.e.*, $\nabla = (\partial_x, 0, 0)$. The first step for this study is to obtain a sufficiently stable slow

134 shock, in order to be able to see the interaction with an Alfvén wave.

135 To determine the needed jumps between the two sides of the shock for all parameters, we
 136 use the Rankine Hugoniot equations. We computed the different possible couples u_{n1}, u_{n2}
 137 for the upstream and downstream normal velocities (see Fig. 9), for any values of the in-
 138 cident magnetic field and pressure. The curve presented on Fig. 9 is for example obtained
 139 for $P_1 = 0.1$, $B_n = 0.1$, $\rho_1 = 1$, and $B_{t1} = 1$.

140 We inject the chosen values $u_{n1} = 0.065$, $u_{n2} = 0.035$ in the simulation code, as the
 141 extreme values of a ramp of u_n with a $\tanh kx$ profile. The width of the shock is of a
 142 few mesh points. To respect the periodic boundary conditions, we add a linear variation
 143 leading the u_n function to the same value on the two boundaries. To initialize all the other
 144 quantities at all points, we directly use the conservation laws of the Rankine-Hugoniot
 145 system.

146 Using this initialization we obtain something which is not perfectly stationary (our equa-
 147 tions do not take account of the code viscosity and the profiles are thus not perfectly
 148 known), but enough to study the interaction with a rotational discontinuity. Fig. 9 shows
 149 the evolution of density and fields for small times. A small perturbation of density seems
 150 to propagate alone on the right on the box (we will see that it does not change the results),
 151 and we observe a small smoothing of the gradients, but the shock is not globally moving.

5.2. Interaction with an Alfvén wave

152 We then add an Alfvén wave in the right side of the simulation box, consisting in a 2π
 153 rotation of the magnetic field, with a Walén consistent rotation of velocity. The subse-
 154 quent evolution after this initialization is shown on Fig. 11 for small times (until $t=15$).
 155 We see that the Alfvén wave is normally propagating on the x direction from right to left

156 and encounters the density gradient around $t=9$. The shock then begins to move with the
157 Alfvén wave instead of remaining steady. The imperfection on the initialization does not
158 play any significant role in this phenomenon.

159 This effect becomes spectacular if we look at the simulation for a longer time. Fig. 12
160 and Fig. 13 show the evolution every 20 seconds during 60 seconds, respectively with the
161 Alfvén wave, and without the Alfvén wave. There is no doubt that we see the formation of
162 a slow shock/rotational discontinuity compound, the slow shock moving with the Alfvén
163 wave. Such a structure is quite reminiscent of the so-called "double discontinuities" de-
164 scribed in (*Whang et al*, 1998). Nevertheless, these structures are usually supposed to be
165 related to an anisotropic (*Lee et al*, 2000) plasma, which is not the case in this MHD code.
166 However, the anisotropy is said necessary to explain the stationarity of this structure. As
167 the observed layer is not strictly stationary, even if it evolves very slowly when the two
168 layers merge, there is no necessary contradiction.

169 This kind of structure is forbidden by MHD equations if it has to be stationary, but it
170 is not, at least at times we can reach with the simulation, as shown on Fig. 14 that shows
171 the respective positions of the B_z and density gradients at different times. The shock
172 affects the shape of the rotation of magnetic field (even if a Walén test can show it is still
173 Alfvénic), and the compressional part position seems to be oscillating.

174

6. Conclusion

175 We have presented a case study of a magnetopause crossing by Cluster spacecraft.
176 This example is atypical in the sense that the density/ temperature gradient is clearly
177 separated from the magnetic field rotation layer. This allows to investigate separately

178 the two layers and determine their nature. Using a new method, the normal direction is
179 determined with a good accuracy and the normal components B_n of the magnetic field
180 and u_n of the velocity can be measured in a reliable way: the two layers are not tangential.
181 In addition, the method allows plotting the different profiles in function of a transition
182 parameter which is a trustworthy proxy of a normal coordinate. The density/temperature
183 gradient layer could so be identified unambiguously as a slow shock, while the rotation
184 layer has all the properties of a rotational discontinuity, except that it may propagate at
185 $0.7 V_A$ instead of V_A . A 1,5 D MHD simulation has been performed to investigate the
186 interaction between a slow shock and a rotational discontinuity when they meet. The
187 results are quite comparable with the data : The shock stays attached to the rotational
188 discontinuity, at least before viscosity kills all the gradients in the simulation, and keeps
189 shock properties as the second part of the discontinuity is still rotational. The structure
190 is not stationary and so stays compatible with MHD equations. We can conjecture that
191 this kind of interaction between compressional and rotational features is a generic feature
192 of the magnetopause.

193 **Acknowledgments.** The authors would like to thank the CAA and all Cluster instru-
194 ments teams for their work on Cluster data.

References

195 Balogh, A., Dunlop, M. W., Cowley, S. W. H., Southwood, D. J., Thomlinson, J. G., and
196 the Cluster magnetometer team: The Cluster magnetic field investigation, *Space Sci.*
197 *Rev.*, 79, 65, 1997

- 198 Chou, Y.-C. and L.-N. Hau (2012), A statistical study of magnetopause structures: Tan-
199 gential versus rotational discontinuities, *J. Geophys. Res.*, doi:10.1029/2011JA017155,
200 in press.
- 201 Dorville, N. et al, BV technique for investigating 1-D interfaces, submitted to *JGR*, 2013
- 202 Lee, L. C., B. H. Wu, J. K. Chao, C. H. Lin, and Y. Li (2000), Formation of a compound
203 slow shock-rotational discontinuity structure, *J. Geophys. Res.*, 105(A6), 1304513053,
204 doi:10.1029/2000JA900011.
- 205 Neugebauer, M., Clay, D. R., Goldstein, B. E., and Tsurutani, B. T., A reexamination
206 of rotational and tangential discontinuities in the Solar Wind, *J. Geophys. Res.* 89,
207 5395-5408, 1984
- 208 Paschmann, G., and Sonnerup, B. U. ., 2008, Proper Frame Determination and Waln
209 Test, in *Multi-spacecraft Analysis Methods Revisited*, edited by G. Paschmann and P.
210 W. Daly, no. SR-008 in *ISSI Scientific Reports*, chap. 7, pp. 69-71, ESA Publ. Div.,
211 Noordwijk, Netherlands.
- 212 Rème, H., Cottin, F., Cros, A., et al.: The Cluster Ion Spectrometry (CIS) Experiment,
213 *Space Sciences Review* 79, 303-350, 1997
- 214 Sonnerup, B. U., and B. G. Ledley (1974), Magnetopause rotational forms, *J. Geophys.*
215 *Res.*, 79(28), 43094314, doi:10.1029/JA079i028p04309.
- 216 Sonnerup, B. U. ., and Scheible, M., 1998, Minimum and Maximum Variance Analysis, in
217 *Analysis Methods for Multispacecraft Data*, edited by G. Paschmann and P. W. Daly,
218 no. SR-001 in *ISSI Scientific Reports*, chap. 8, pp. 187-196, ESA Publ. Div., Noordwijk,
219 Netherlands.

220 Whang, Y. C. et al., Double discontinuity: A compound structure of slow shock and
 221 rotational discontinuity, J. Geophys. Res.,103, 6513, 1998.

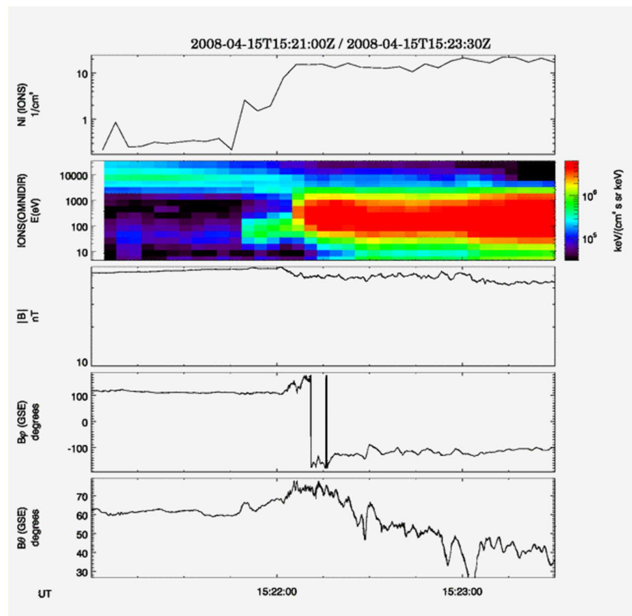


Figure 1. Density, energy spectrogram and magnetic field observed by Cluster C1 around 15:21 on 04/15/2008. The jump of density, change in plasma energy composition and rotation of magnetic field show that the satellite is crossing the magnetopause.

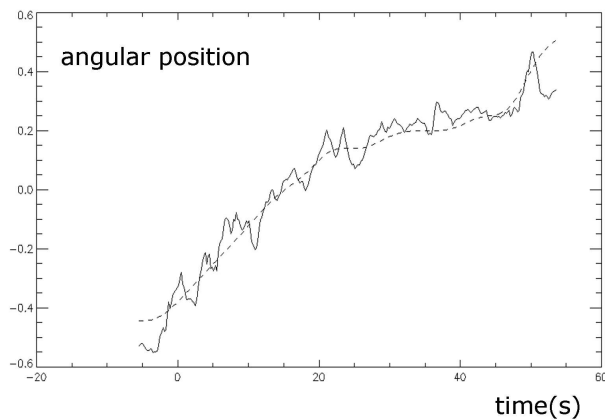


Figure 2. Observed angle on the elliptic hodogram and fit (dashed line) derived with CIS velocity by the BV method as a function of time for Cluster C1 crossing of 04/15/2008.

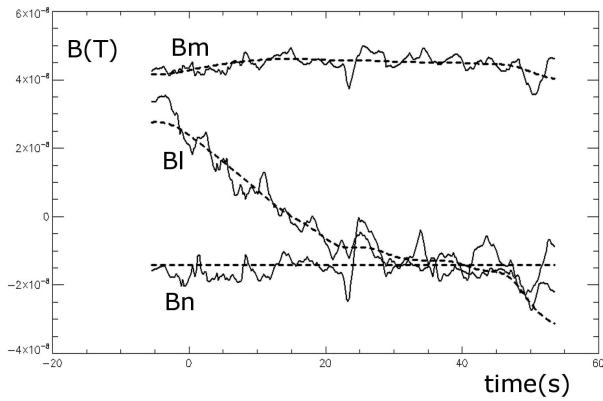


Figure 3. Three components of the magnetic field data measured by FGM and fit (dashed line) by the BV method in the magnetic field rotation region for Cluster C1 crossing of 04/15/2008.

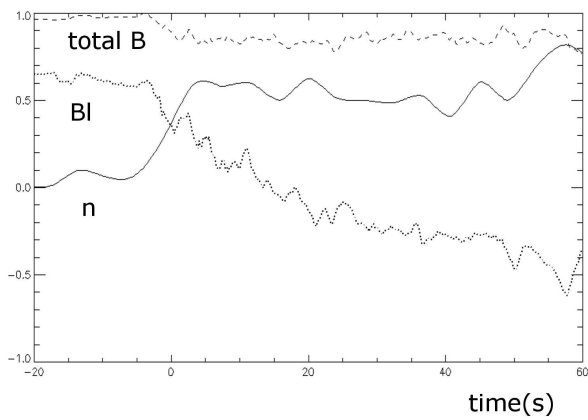


Figure 4. Time evolution of density, total magnetic field and B_L component of the magnetic field during the for Cluster C1 magnetopause crossing of 04/15/2008.

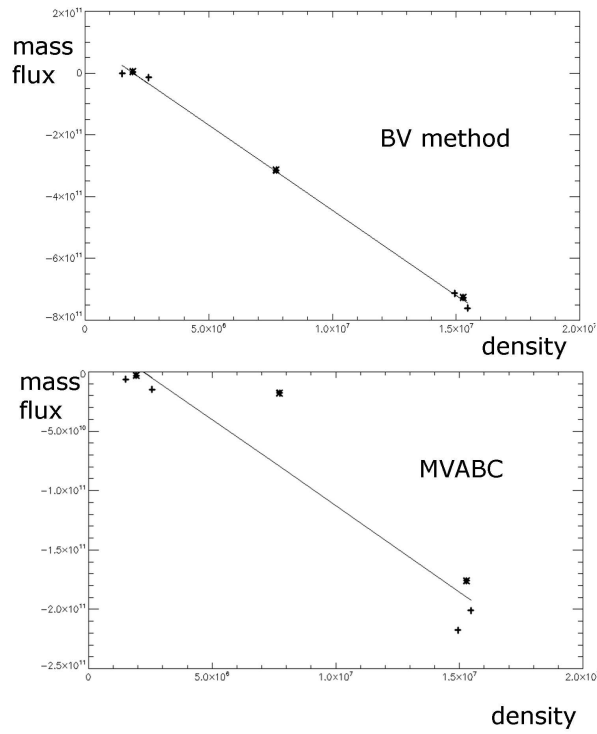


Figure 5. The normal mass flux in the shock (stars) and around it (crosses) for the BV method improved frame and in the MVABC frame. The proportionality in the BV frame shows that it is considerably better and permits to deduce the shock velocity with respect to the spacecraft.

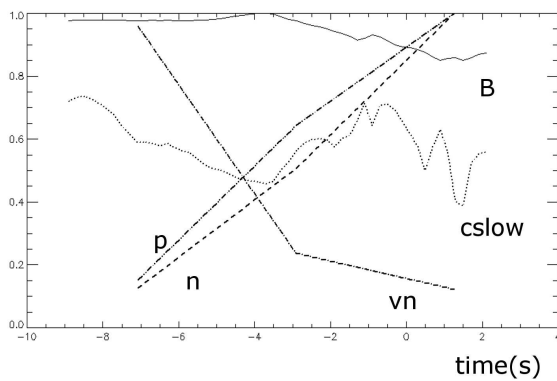


Figure 6. Normal velocity, density, pressure, magnetic field modulus and slow mode velocity as a function of time for the shock.

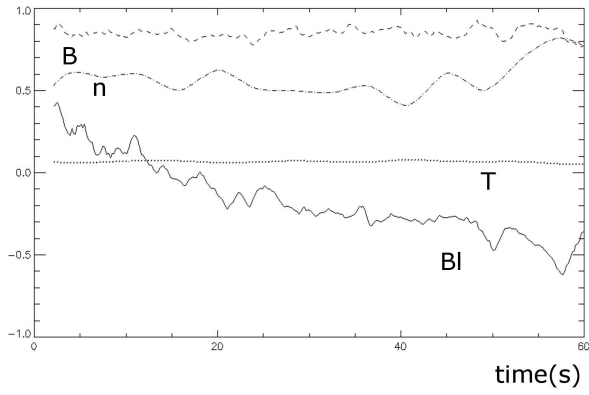


Figure 7. B_L component of magnetic field, density, temperature, and magnetic field modulus as a function of time for the rotational discontinuity.

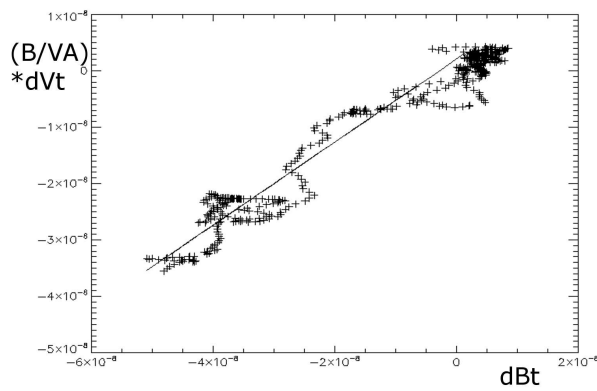


Figure 8. Variant of the Walen test for the rotational discontinuity, $\frac{B}{V_a} * dV_t$ is represented over dB_t .

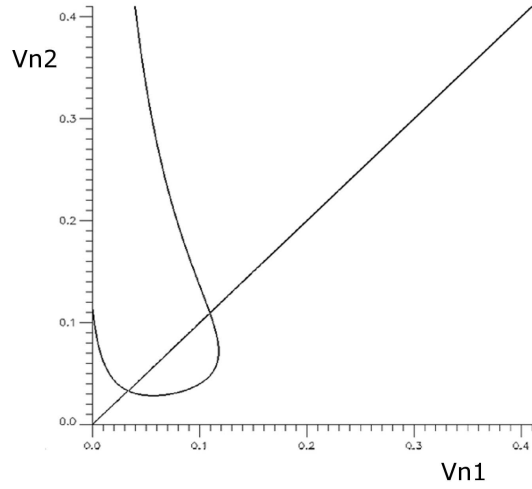


Figure 9. Possible couples of normal velocity boundary conditions allowed by Rankine-Hugoniot equations ($Vn2$ as a function of $Vn1$).

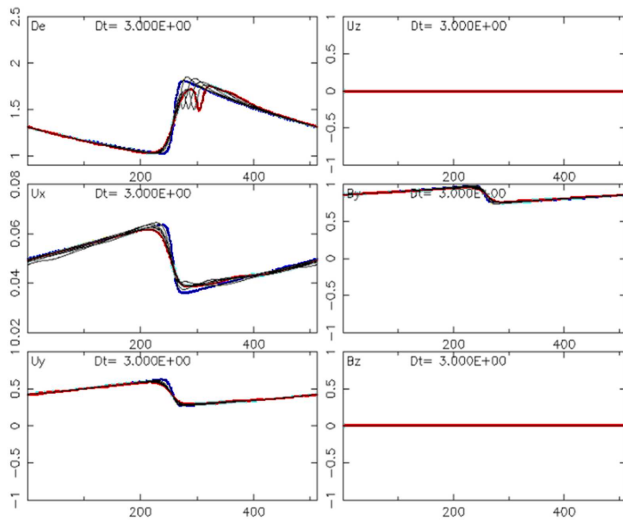


Figure 10. Early evolution of plasma parameters from the initialization (blue curve) to the last time step (red curve) for the shock initialized alone in the box.

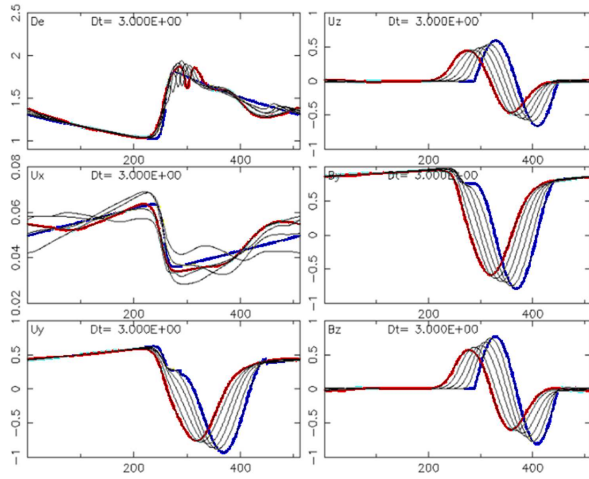


Figure 11. Early evolution of plasma parameters from the initialization (blue curve) to the last time step (red curve) when a rotational discontinuity is added in the initial condition next to the shock.

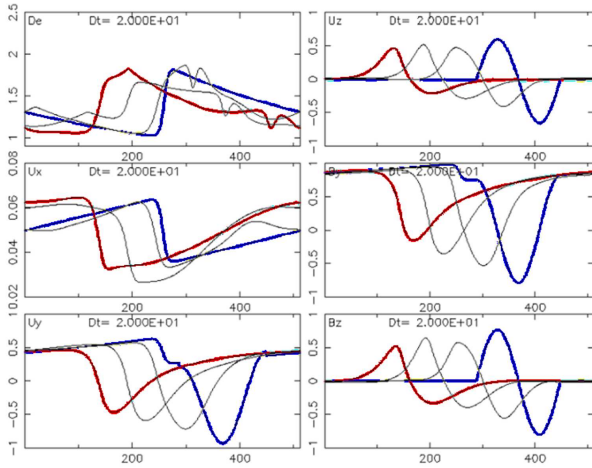


Figure 12. Long time evolution of plasma parameters from the initialization (blue curve) to the last time step (red curve) when a rotational discontinuity is added in the initial condition next to the shock.

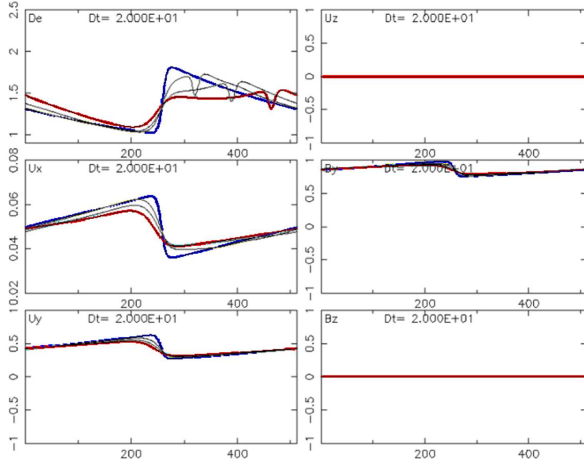


Figure 13. Long time evolution of plasma parameters from the initialization (blue curve) to the last time step (red curve) for the shock initialized alone in the box.

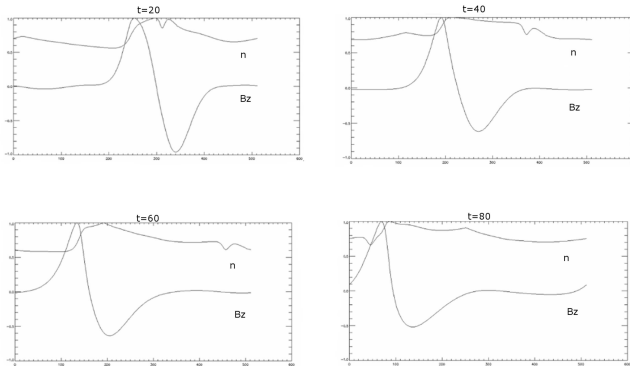


Figure 14. Shock and rotation discontinuity positions at different times. The density is used as a proxy for the shock and the Bz component as a proxy for the rotational discontinuity. The structure is not stationary.